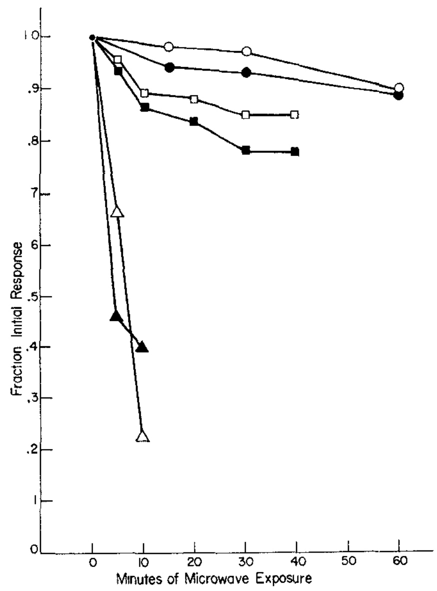

Fig. 1. Effect of microwaves on TL response of powder and ceramic phosphors. Error bars are not shown, but standard error of the mean averaged 0.068. (○—○), $(Ba_{0.8}Sr_{0.2})TiO_3$ stored at room temperature; (●—●), $(Ba_{0.8}Sr_{0.2})TiO_3$ stored at elevated temperature; (□—□), $(Ba_{0.8}Sr_{0.2})TiO_3$ powder exposed to 200 mW/cm^2; (■—■), $(Ba_{0.8}Sr_{0.2})TiO_3$ powder exposed to approximately 5000 mW/cm^2, (△—△), $BaTiO_3$ ceramic, (▲—▲), $(Ba_{0.8}Sr_{0.2})TiO_3$ ceramic. Results of the microwave exposures were normalized to the control to obtain fraction of initial response (no microwave exposure). Results of the elevated (28°C) exposure were not normalized in order to compare them directly with a control (22°C). In the latter comparison the zero time is a phosphor sample stored on dry ice and receiving no exposure to room temperature or to elevated temperature.

luminescence. However, the fading observed at 28°C was significantly ($P<0.05$) less than the fading observed after microwave exposure (Fig. 1). Since an increase in phosphor temperature alone did not account for all the fading, a significant amount of the fading in $(Ba_{0.8}Sr_{0.2})TiO_3$ after microwave exposure may have been due to a nonthermal or "microthermal" interaction.

The polyethylene vials containing the TSEE phosphors began to melt after 1 min of microwave oven exposure suggesting a phosphor temperature of 60–70°C. No temperature fading study was conducted, and it was concluded that the fading seen was strictly thermal.

From a practical point of view, the use of a ceramic and the fading effects seen in the ceramic are of more interest than use of the powdered materials. This interest is due to several reasons, the most significant of which are the more exact knowledge of dielectric properties of the ceramic versus that of powder, and larger values of dielectric constant and loss tangent for the ceramic than the powder. Furthermore, a solid piece is more easily handled than a quantity of loose powder and can be formed in a specific shape before firing. The ceramics were produced from the activated phosphors of $BaTiO_3$ containing 0, 0.1, and 0.5 mole percent Dy, and the combination powder $(Ba_{0.8}Sr_{0.2})TiO_3$. Preirradiated ceramics showed a marked reduction in TL response when compared to a control stored at room temperature (Fig. 1). Because of the difficulty in determining the temperature of a ceramic during or immediately after microwave exposure, a higher-than-room-temperature control was not used. However, the ceramics were not warm to the touch following the microwave exposure.

Ceramic pieces 2 cm or more in length, were placed on a Styrofoam support in the anechoic chamber after ^{60}Co irradiation and exposed to microwaves in a manner similar to the powder samples. Accurate determination of the effect of microwave exposure required multiple readouts of the same ceramic piece. After each readout, the ceramic was annealed for 30 min at 400°C and cooled to room temperature, then reirradiated with ^{60}Co, exposed to microwaves, and read out. Because a limited number of ceramics was available, only the high power density of approximately 5000 mW/cm^2 was used to test for TL fading. The reduction in response was energy fluence dependent; that is, the longer the microwave exposure, the greater the fading. The Dy-activated $BaTiO_3$ ceramics faded at approximately the same rate as the $(Ba_{0.8}Sr_{0.2})TiO_3$ ceramic but for clarity were not plotted in Fig. 1. Because of the preliminary nature of this study, the power density used was admittedly high with respect to personnel safety considerations. It is suggested that ceramics production and phosphor activation be optimized before more reasonable power densities are used.

IV. Conclusions

The results of these studies, using both powders and ceramics, show microwave-induced TL fading to be energy fluence dependent, with increasing microwave exposure time resulting in decreased TL response. Further, most of the fading observed after microwave exposure is probably due to some interaction other than thermal. A mechanism of action is not suggested at this time, but it is suggested that the fading phenomenon observed in these studies may provide a method of microwave dosimetry. No microwave-induced fading was observed in TSEE phosphors except when they were mixed with graphite and exposed to extremely high power densities. It was concluded that the TSEE fading observed was completely thermal in nature.

Acknowledgment

The authors wish to thank D. L. Conover for designing the anechoic chamber used in this study.

References

[1] S. M. Michaelson, "Biological effects of microwave exposure—An overview," *J. Microwave Power*, vol. 6, pp. 259–267, 1971.
[2] D. I. McRee, "Environmental aspects of microwave radiation," *Environ. Health Perspect.*, pp. 41–52, Oct. 1972.
[3] D. L. Conover, "Evaluation of lithium fluoride for microwave dosimetry application," U. S. Dep. Health, Ed. and Welf., Rep. BRH/DEP 71-6, Apr. 1971.
[4] F. Daniels, "Early studies of thermoluminescence radiation dosimetry," in *Proc. Int. Conf. Luminescence Dosimetry*, F. A. Attix, Ed. (Stanford, Calif.), Apr. 1967, pp. 34–43.
[5] K. Becker, "Principles of thermally stimulated exoelectron emission (TSEE) dosimetry," *IAEA At. Energy Rev.*, vol. 8, p. 173, 1970.
[6] D. R. Elle, "Thermoluminescence and microwave induced thermoluminescent fading of high dielectric constant inorganic materials," Ph.D. dissertation, Purdue Univ., Lafayette, Ind., Dec. 1972.
[7] D. J. Fehringer, "The effects of microwave radiation on thermally stimulated exoelectron emission," M.S. thesis, Purdue Univ., Lafayette, Ind., May 1973.
[8] R. H. Wallace and P. L. Ziemer, "Studies on the thermoluminescence of manganese-activated lithium borate," in *Proc. 2nd Int. Conf. Luminescence Dosimetry* (Gatlinburg, Tenn.), Sept. 1968, pp. 140–147.
[9] P. L. Ziemer, W. C. McArthur, V. L. McManaman, and G. D. Smith, "Characteristics of selected phosphors for stimulated exoelectron emission dosimetry," in *Proc. 3rd Int. Conf. Luminescence Dosimetry*, Danish AEC, Riso, Roskilde, Denmark, RISO Rep. 249, 1972.

Environmentally Controlled Waveguide Irradiation Facility

HENRY S. HO, MEMBER, IEEE, EDWARD I. GINNS, AND CHRISTOPHER L. CHRISTMAN, MEMBER, IEEE

***Abstract*—Research has shown that the determination of absorbed microwave energy as well as the control of environmental parameters are important in relating biological-effect data to radiation protection. This short paper describes the development of an environmentally controlled waveguide irradiation facility for the exposure of small animals to 2450-MHz CW microwave energy. Integral dose rate is determined without perturbing the microwave field interacting with the irradiated animal.**

Glossary

Exposure Rate: Incident power density (mW/cm^2) of an EM wave.

Integral Dose Rate: Time rate of absorption of EM energy (W) by the entire biological body.

Integral Dose: Total amount of EM energy (J or cal) absorbed by the entire biological body.

Average Dose: Integral dose per unit weight of the animal (J/g or cal/g).

Distributed Dose Rate: Time rate of absorption of microwave energy per unit mass (W/kg or W/g). It is usually nonuniform in biological bodies even though the incident power density (exposure rate) may be uniform.

Manuscript received May 10, 1973; revised August 8, 1973.
The authors are with the Division of Biological Effects, Bureau of Radiological Health, FDA, USPHS, Rockville, Md. 20852.

I. Introduction

In the past, the significance of experiments on the biological effects of microwaves to radiation protection has been severely limited by the lack of quantification of the microwave energy absorbed by the irradiated animal. Furthermore, in some cases the interpretation of biological-effect data obtained from exposures without controlled environmental conditions is extremely difficult.

Studies using tissue-equivalent models or phantoms have shown that for both far-field [1]–[3] and near-field [4], [5] exposures, the amount of microwave energy absorbed by a biological body is dependent on the geometry, size, orientation, and complex dielectric constant of the specimen. For a given exposure rate, different animals could therefore receive different dose rates. The spatial distribution of absorbed microwave energy (distributed dose rate) in a test animal is also of importance since hot spots could occur in vital organs under certain exposure conditions [6], [3]. Since dose rate is more directly related to biological effects than exposure rate, the determinations of both the distributed and the integral dose rate in animal experiments are important.

The extent of heat stress in animal systems during microwave irradiation has been evaluated by several workers [7]–[9]. Haines and Hatch [8] as well as Belding and Hatch [7] proposed that heat loss or heat gain due to convection, the subject's metabolic rate, and the heat gain due to radiation, all contribute to the actual heat load experienced by the subject in a microwave field. In an effort to quantitatively describe the physiologically stressed state of a standard man in a microwave field, Mumford [9], [10] derived values for the Heat-Stress Index (HSI) as a function of the Temperature–Humidity Index (THI) and power density. Using rabbits, dogs, mice, and rats, Diechmann [11] further investigated the relationships between an animal's survival in a microwave field and the temperature, humidity, and airflow of the environment. Environmental conditions can influence the extent of strain upon an animal in a microwave field and therefore meaningful microwave biological-effect data must be obtained from exposure situations where the possible environmental variables have been well defined.

This short paper describes the development of an environmentally controlled microwave waveguide irradiation facility for the exposure of small animals such as mice, hamsters, and small rats under controlled environmental conditions. The total amount of microwave energy absorbed by the animal (integral dose) is determined without perturbing the microwave field interacting with the irradiated animal. The time rate of absorption of microwave energy by the animal (integral dose rate) can also be continuously recorded during the experiment.

II. Waveguide Irradiation Facility

The schematic diagram of the waveguide assembly is shown in Fig. 1. The generator provides up to 100 W of CW power at 2450 MHz. The output power is fed through a four-port variable attenuator which controls the amount of power to be fed into the animal chamber. An isolator absorbs the power reflected from the animal chamber and hence isolates the generator. The waveguide unit is a WR 430 waveguide with a 4.3 by 2.15 in cross section. It is designed to operate at the TE_{10} mode within the frequency range of 1.7–2.6 GHz. The powers fed into, P_f, and reflected from, P_r, the specimen are measured through coaxial directional coupler Number 1 by two power meters. The power transmitted through the animal, P_t, is measured through waveguide directional coupler Number 2 by another power meter. The waveguide terminates in a resistive load which absorbs the transmitted power.

Within the waveguide the test animal is free to move within a holder (4.30 by 4.50 by 2.15 in) made of low-loss materials (0.020-in low-density polyethylene, $\epsilon_r = 2.25$, $\tan \delta = 0.0031$; and 0.25-in Styrofoam, $\epsilon_r = 1.03$, $\tan \delta = 0.00010$). Holes in the ends of the holder permit air to flow past the animal. In order to prevent the animal from escaping from the holder, the inside surfaces of the holder are coated with red pepper. In order to facilitate experimentation with animals, the waveguide assembly is mounted on casters and the center section of the waveguide is equipped with quick-release clamps.

Fig. 2 shows the dimensions of the waveguide with a rectangular coordinate system. The exposure condition inside the waveguide in the absence of the animal and holder is shown in the Appendix. In this condition, the reflected power is negligible and the transmitted power is very nearly equal to the forward power. The exposure conditions are described in terms of the electric and magnetic fields and

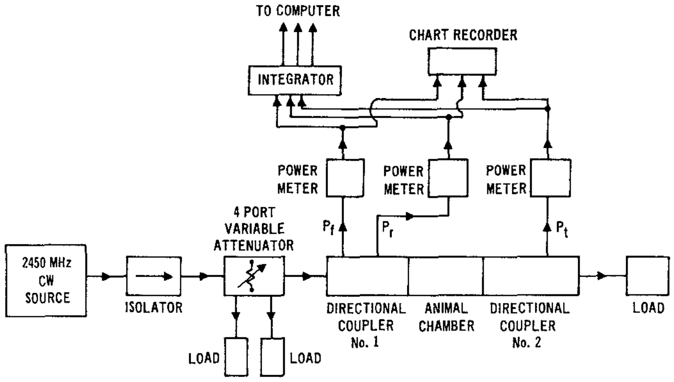

Fig. 1. Schematic diagram of the waveguide irradiation apparatus.

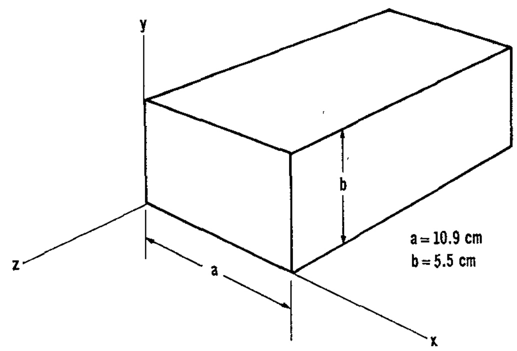

Fig. 2. Cross section of the waveguide with rectangular coordinates.

also the exposure rate (incident power density). The magnitude of the exposure rate can be related to the forward power. Although the exposure rate along the long side of the waveguide has a sine-squared dependence, the exposure rate is uniform along the short side.

Calorimetric testings and theoretical considerations indicate that the power loss to the waveguide walls and the dielectric holder is negligible. The integral dose rate $\dot{\mathcal{E}}$ is therefore

$$\dot{\mathcal{E}} = P_f - (P_r + P_t) \text{ W}. \quad (1)$$

The integral dose rate is found to vary with the movement of the test animal. This variation is caused by the changes in the reflected and transmitted powers. In order to determine the integral dose, analog voltage outputs from the three power meters are fed into an integrator of our design and construction. Each of the power readings is integrated with respect to time, and the integral dose absorbed by the animal is expressed as

$$\mathcal{E} = \int_0^T P_f dt - \left[\int_0^T P_r dt + \int_0^T P_t dt \right] \text{ J} \quad (2)$$

where $\mathcal{E}$ is the integral dose, and T is the exposure time. The analog integrator also provides analog output signals so that the forward, reflected, and transmitted powers can be monitored continuously on a chart recorder.

III. Exposure Environment

It has been known for some time that environmental conditions influence the extent of strain on a subject in a microwave field. To ensure reproducibility in experiments, the chamber shown schematically in Fig. 3 was constructed to contain the microwave apparatus. Temperature, relative humidity, and airflow past the animal are specified during an exposure. As seen from Fig. 3, the environment within the chamber is obtained by mixing two air streams—one that has been cooled and dehumidified and one that has been heated and humidified.

The air temperature is measured with a protected thermocouple probe (thermocouple telethermometer) located at the center of the chamber just above the waveguide. The fluctuation in temperature during an exposure is less than ±0.5°C. The variation in relative

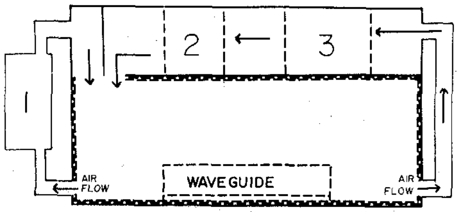

Fig. 3. Schematic illustration of the environmental chamber housing the microwave waveguide irradiation apparatus. 1) Air conditioner. 2) Heater. 3) Humidifier.

humidity (measured with a membrane hygrometer at the air inlet of the waveguide) is ± 1.5 percent during an exposure. The range of relative humidity that can be obtained within the chamber is 25–70 percent over the temperature range of 15–40°C. Using the following equation [9]:

$$\text{THI} \doteq 1.44T + 0.1\text{RH} + 30.6 \qquad (3)$$

(where T=temperature, °C; RH=relative humidity) the environmental chamber provides a range of THI from 55 to 95.

The temperature and moisture conditioned air within the environmental chamber is drawn through the waveguide by a low-pressure (vacuum) system attached to one end of the waveguide. The 0.25-in air-inlet and air-outlet openings at the ends of the waveguide have no effect on dosimetry. Airflow rates (past the animal being irradiated) of up to 38 l/min (measured with an air-calibrated flowmeter) are possible. The front of the chamber is fitted with gloves that permit access to the interior of the chamber without disturbing the controlled environment.

IV. Results

The irradiation facility described in this short paper permits the exposure of an animal in a controlled environment where the animal is not anesthetized or drastically constrained (e.g., tied down). It appears that such an exposure condition (free to move) is more desirable than one where the animal is more restricted in its movements and where it is probably more strained. In control studies, CF1 mice weighing approximately 35 g showed no rise in rectal temperature after being confined in this irradiation facility for periods in excess of 3 h.

Since the animal is free to move within the holder during an exposure, the reflected and transmitted powers are varying. A typical pattern of power variation (reflected power) during an exposure is illustrated in Fig. 4. The ordinate corresponds to the analog output from the power meter. By recording such an "activity indicator" during an exposure, we are able to monitor the physiological state of an animal. This activity indicator further provides a means of investigating the sensitivity of an animal to both environmental and dosimetric (e.g., dose rate) parameters for which lethality can be used as an endpoint. The time of death of the irradiated animal can be precisely determined and the average dose can subsequently be calculated.

The relationship between the integral dose and animal weight for CF1 mice exposed to 2450-MHz microwaves in the waveguide apparatus is shown in Fig. 5. The data indicate that a heavier mouse has a higher integral dose than a small mouse. Fig. 6, however, shows that the average dose for the same group of mice is less for the heavier mice. These results can be compared to the theoretical calculations of integral dose for a 3-cm- and a 15-cm-radius muscle sphere exposed to plane-wave EM radiation as shown in Fig. 7 [3]. The integral dose rate of the larger (heavier) sphere is greater than that of the smaller sphere, but the average dose rate of the smaller sphere is greater than that of the larger sphere. Thus the theoretical treatment of muscle equivalent spheres and the results obtained in the waveguide irradiation of CF1 mice are consistent with one another.

V. Conclusion

It appears that the specification of exposure rate alone is not dosimetrically sufficient for relating the results of biological-effect experiments to radiation protection. The meaningful interpretation of biological-effect data is also dependent on the precise definition of the exposure environment. This short paper describes an environmentally controlled facility that permits the determination of integral dose.

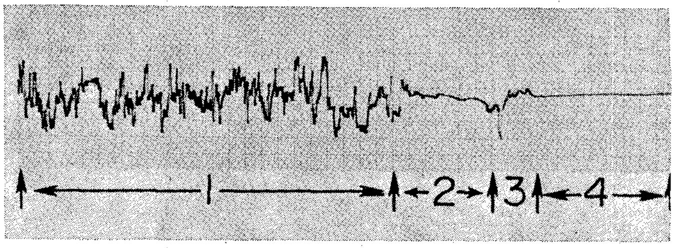

Fig. 4. Activity indicator for a CF1 mouse moving in an intense microwave field. Chart speed: 0.5 mm/s. (Ordinate is a voltage reading corresponding to reflected power; abscissa represents time coordinates of exposure, where each major division corresponds to 10 s; forward power is 8.36 W). Phase 1—transition from unstressed to stressed state. Phase 2—fatigued and labored movement. Phase 3—convulsive movement. Phase 4—death.

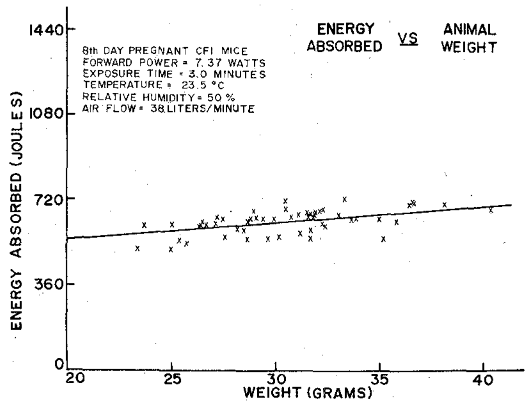

Fig. 5. Measured integral dose (energy absorbed) versus weight of animal for a fixed forward power.

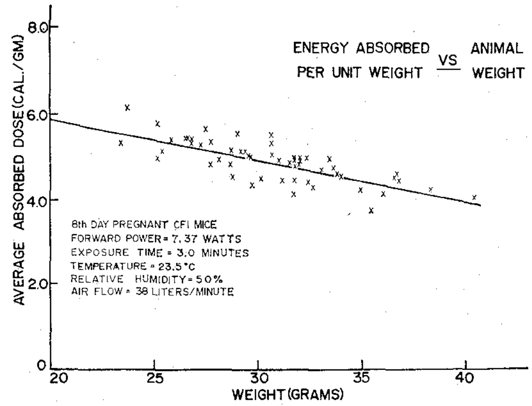

Fig. 6. Measured average dose versus weight of animal for a fixed forward power.

Future work will use the thermographic technique [4] in the determination of distributed dose rate information. The dose-biological-effect data thus obtained can be dosimetrically related to radiation protection guides (in terms of exposure rate) by the additional determination of integral and distributed dose in human or phantom bodies.

Appendix

Exposure Conditions

$$E_y = E_+ e^{-j\beta z} \sin(\pi x/a)$$

$$H_x = -(\beta/\omega\mu) E_y$$

$$H_z = -(\pi/a)(E_+/j\omega\mu) e^{-j\beta z} \cos(\pi x/a)$$

$$\dot{X}(\text{exposure rate}) = (1/2)\,\text{Re}\,|E \times H^*|$$

$$= \dot{X}_0 \sin^2(\pi x/a)$$

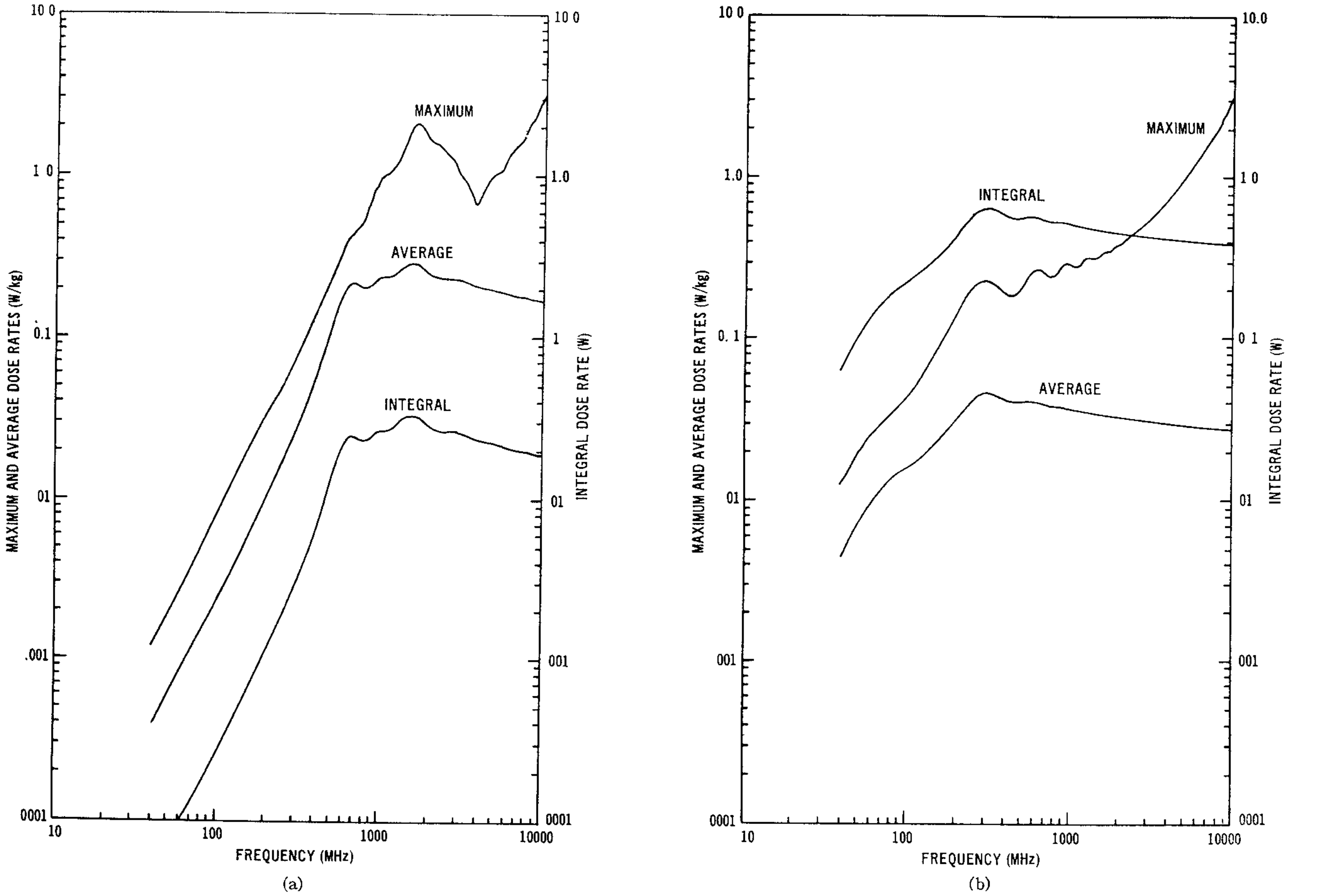

Fig. 7. Frequency dependencies of maximum, average, and integral dose rates in muscle equivalent spheres of (a) 3-cm and (b) 15-cm radii for incident monochromatic plane waves with exposure rate of 1 mW/cm².

where

$$\beta = \{\omega^2\mu\epsilon - (\pi/a)^2\}^{1/2}$$
$$Z_0 = [\{\epsilon/\mu\}\{1 - (\lambda/2a)^2\}]^{-1/2}$$
$$E_+ = (4P_f Z_0/ab)^{1/2}$$
$$\dot{X}_0 = 2P_f/ab$$

P_f forward power into the waveguide

λ wavelength

μ, ϵ permeability, permittivity

$\omega = 2\pi f$

f source frequency.

The preceding are exposure conditions of a waveguide operating in TE_{10} mode (with matched load and in the absence of the animal).

Acknowledgment

The authors wish to thank K. M. Selby and N. J. Cochran for their assistance in animal experiments and data collection, and W. Ridgley and K. T. Armentrout for their assistance in the construction of the facility.

References

[1] J. P. Schwan, "Interaction of microwave and radio frequency radiation with biological systems," in *Proc. Biological Effects and Health Implications of Microwave Radiation* (Richmond, Va., Sept. 17–19, 1969), pp. 13–20.

[2] H. P. Schwan, A. Anne, M. Saito, and O. M. Salti, "Relative microwave absorption of cross sections of biological significance," in *Proc. 4th Conf. Biological Effects of Microwave Radiation*, vol. 1. New York: Plenum, 1961, pp. 153–176.

[3] H. S. Ho and H. D. Youmans, "The dosimetry of VHF-SHF electromagnetic fields," in *Proc. 1972 Fall USNC/URSI Meeting* (Williamsburg, Va., Dec. 11–15, 1972).

[4] A. W. Guy, "Analyses of electromagnetic fields induced in biological tissues by thermographic studies on equivalent phantom models," *IEEE Trans. Microwave Theory Tech.*, vol. MTT-19, pp. 205–214, Feb. 1971.

[5] H. S. Ho, A. W. Guy, R. A. Sigelmann, and J. F. Lehmann, "Microwave heating of simulated human limbs by aperture sources," *IEEE Trans. Microwave Theory Tech.*, vol. MTT-19, pp. 224–231, Feb. 1971.

[6] A. R. Shapiro, R. F. Lutomirski, and H. T. Yura, "Induced fields and heating within a cranial structure irradiated by an electromagnetic plane wave," *IEEE Trans. Microwave Theory Tech.*, vol. MTT-19, pp. 187–196, Feb. 1971.

[7] H. S. Belding and T. F. Hatch, *Heat. Piping, Air Cond.*, p. 129, Aug. 1955.

[8] G. F. Haines, Jr., and T. F. Hatch, *Heat. Vent.*, Nov. 1952.

[9] W. W. Mumford, "Heat stress due to RF radiation," *Proc. IEEE*, vol. 57, pp. 177–178, Feb. 1969.

[10] S. F. Cleary, Ed., *Symp. Proc. Biological Effects and Health Implications o Microwave Radiation*, BRH/DBE, 1970, p. 21.

[11] W. B. Diechmann, *Archiv. Für Toxikologie*, vol. 22, pp. 24–35, 1966.

High-Power *S*-Band Junction Circulator

R. A. STERN, MEMBER, IEEE

***Abstract*—The design of a high-power air-cooled microwave Y-junction circulator which is capable of operation at peak and average power levels of 800 kW and 800 W, respectively, is described. The unit is an *H*-plane waveguide circulator which is externally air cooled. The circulator design employs a full-height substituted YIG rod with a center metal pin together with boron nitride matching transformers.**

The circulator exhibits an insertion loss of less than 0.4 dB, isolation greater than 22 dB, and a VSWR < 1.26:1 over a 400-MHz bandwidth centered at 3.3 GHz. At high-power levels, the device exhibits insertion loss of less than 0.9 dB, isolation greater than 20 dB, and VSWR < 1.25:1 at an indicative frequency within the operating bandwidth.

Manuscript received May 7, 1973, revised August 3, 1973.
The author is with the Microwave and Acoustics Devices Team, Frequency Control and Signal Processing Devices Technical Area, Department of the Army, U. S. Army Electronics Command, Fort Monmouth, N. J. 07703.